PNAS
www.pnas.org

Supplementary Information for

Three-micrometer-diameter needle electrode with an amplifier for extracellular in vivo recordings

Yuto Kita[a], Shuhei Tsuruhara[a], Hiroshi Kubo[a], Koji Yamashita[a], Yu Seikoba[a], Shinnosuke Idogawa[a], Hirohito Sawahata[a, b], Shota Yamagiwa[a], Xian Long Angela Leong[a], Rika Numano[c], Kowa Koida [d, e] and Takeshi Kawano[a, *]

[a] Department of Electrical and Electric Information Engineering, Toyohashi University of Technology, 1-1 Hibarigaoka Tempaku-cho, Toyohashi 441-8580, Japan

[b] National Institute of Technology, Ibaraki College, 866 Nakane, Hitachinaka 312-8508, Japan

[c] Department of Applied Chemistry and Life Science, Toyohashi University of Technology, 1-1 Hibarigaoka Tempaku-cho, Toyohashi 441-8580, Japan

[d] Department of Computer Science and Engineering, Toyohashi University of Technology, 1-1 Hibarigaoka Tempaku-cho, Toyohashi 441-8580, Japan

[e] Electronics-Inspired Interdisciplinary Research Institute (EIIRIS), Toyohashi University of Technology, 1-1 Hibarigaoka Tempaku-cho, Toyohashi 441-8580, Japan

*Correspondence and requests for materials should be addressed to

Takeshi Kawano, Department of Electrical and Electric Information Engineering, Toyohashi University of Technology, 1-1 Hibarigaoka Tempaku-cho, Toyohashi 441-8580, Japan,

Telephone: +81(532)-44-6738; FAX: +81(532)-44-6757

Email: kawano@ee.tut.ac.jp

This PDF file includes:

Supplementary text
Figures S1 to S9
SI References

Supplementary Information Text

Text ST1. Elimination of voltage attenuation of neuronal signal with source follower

A high impedance electrode induces voltage attenuation of neuronal signals which can be eliminated with source follower configuration. As shown in the equivalent circuit model (Fig. S1*A*), the neural recording via the microneedle without assembling amplifier module yields a voltage divider configuration associated with the electrode impedance [5 MΩ at 1 kHz (1)] and the parasitic impedance of the recording cable between the electrode and the recording amplifier (ZC64, TDT, input impedance = 1×10^{14} Ω). The voltage divider configuration in the recording system causes voltage attenuation of neuronal signals detected at the electrode [e.g., > 40 % attenuation (1)].

To avoid this, we used an amplifier module consisting of a source follower, which plays a role in the transformation of the electrode's impedance to the output impedance of the drive MOSFET in the source follower. Fig. S1*B* shows the small-signal model of the source follower. The output resistance of the source follower, Z_{out}, is given by:

$$Z_{out} = \frac{v_{out}}{i_{out}} = \frac{1}{g_m + \frac{1}{r_o} + \frac{1}{R_{load}}}$$

$$= \frac{r_o \,//\, R_{load}}{g_m(r_o \,//\, R_{load}) + 1}$$

where i_{out} is current from the output terminal, g_{m} is transconductance of the MOSFET, and $r_o \,//\, R_{load} = r_o R_{load}/(r_o + R_{load})$. Since, $g_m(r_o \,//\, R_{load}) \gg 1$, we obtain Z_{out},

$$Z_{out} \simeq \frac{1}{g_m}.$$

Having parameters of the used NMOS, we calculate $1/g_m = 7.4$ kΩ (<< electrode impedance, 5 MΩ at 1 kHz).

Text ST2. Pharmacological block of neuronal activity

To confirm that the STACK device recorded signals which originated from neurons in the mouse's brain tissue, we conducted neuronal recordings, in which the neuronal activities in the S1B were pharmacologically blocked with lidocaine during the mouse's whisker stimulation. Similar to the in vivo acute recording (Fig. 4), the microneedle-electrode of the STACK device penetrated the primary somatosensory cortex (S1B) in the right hemisphere of an anesthetized mouse (male, 35.7 g in weight, 100 μL of 0.5% solution per 10 g body weight for chlorprothixene and 50 μL of 10% solution per 10 g body weight for urethane). During the recording, the mouse's whiskers were stimulated to evoke the neuronal responses (*Materials and Methods* in Main Manuscript). For the pharmacological block of neuronal activity, we used a 20 mg/ml lidocaine solution, which was typically applied to the S1B in the mouse's right hemisphere (Fig. S7*A*).

Fig. S7*B* shows the recording results of the pharmacological blocking of neuronal activity. The STACK device was enabled to record signals responding to the whisker stimuli in a recording period of 0–11 sec. Fig. S7 *C*, *1* shows the average waveform of low-frequency band signals (filtering = 1–300 Hz, n = 50 trials). The signals were in response to the whisker stimuli with a latency of ~20 ms. Fig. S7 *C*, *2* shows the typical high-frequency band signal (filtering = 500 – 3,000 Hz) recorded with the STACK device trial. Fig. S7 *C*, *3* and *4* depict the raster plot diagram and peristimulus time histogram (PSTH) of these signals, respectively. The detection threshold of these signals were 3× the SD (σ) of the mean signal −0.5 to −1.0 s before stimulus onset. However, these signals were slightly reduced after the application of lidocaine (after 11 sec, "Lidocaine applied" in Fig. S7 *D*, *1–4*). Following lidocaine application, the S1B was washed out with saline for approximately 30 min. After a recording period of about 45 s (Fig. S7 *E*, *1–4*), we observed the recovery of the signals. The observation was replicated with a different mouse. Because these signals responding to the whisker stimuli appeared before and after lidocaine application, these recorded signals via the STACK device represented evoked neuronal responses by the whisker stimulation.

Text ST3. Wireless system configuration

The wireless neuronal recording with the fabricated STACK device was demonstrated herein using a commercially available Bluetooth module as the wireless unit (Fig. S8). The front-end amplifier (source follower, −0.175 dB), STACK device, was followed by a high-pass filter and a 40-dB stage amplifier (LT1167, Linear Technology, noise level = <90 nV/√Hz at 1 kHz) (Fig. S8*A*). We used a high-pass filter after the first −0.175 dB front-end amplifier (source follower, STACK device). The cutoff frequency of the high-pass filter was set at 0.1 Hz (C_1 = 1.5 μF, R_1 = 1 MΩ, Fig. S8*B*) to eliminate the amplitude drifts associated with the electrolyte–metal interfacial properties. A second gain stage added 40 dB of additional gain (R_2 = 470 Ω) to digitise and transmit these neuronal signals with a Bluetooth transmitter (MM-BTAD4N2, Sanwa Supply Inc.). The recorded neuronal signals through the STACK device, 2nd-stage AMP circuit and Bluetooth transmitter were wirelessly transmitted to a Bluetooth receiver (LBT-AVWAR700, Elecom Co., Ltd.). The voltage gain of the wireless recording system (Fig. S8*A*) measured at 500–3,000 Hz was 67 dB, whereas the system without a source follower (−0.175 dB) of the STACK device showed a lower gain of 61 dB (Fig. S8*C*). The high-pass filter pole at 50 Hz was caused by the transfer function of the used Bluetooth transmitter.

A

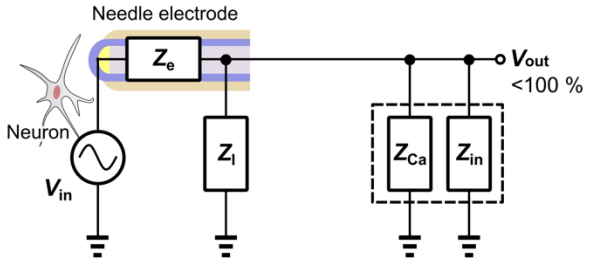

B

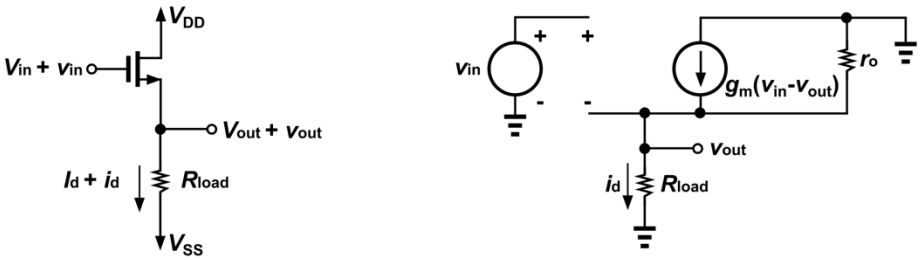

Fig. S1. Equivalent circuit models of needle electrode and source follower: (*A*) Needle electrode in neuronal recording. The recording system between the electrode and the recording amplifier consists of the needle's electrolyte/metal interface electrical impedance, Z_e, and parasitic impedances of device interconnection, Z_l, cable capacitance, Z_{Ca}, and input impedance of the amplifier, Z_{in}, yielding a voltage divider configuration. (*B*) Source follower and the small signal model.

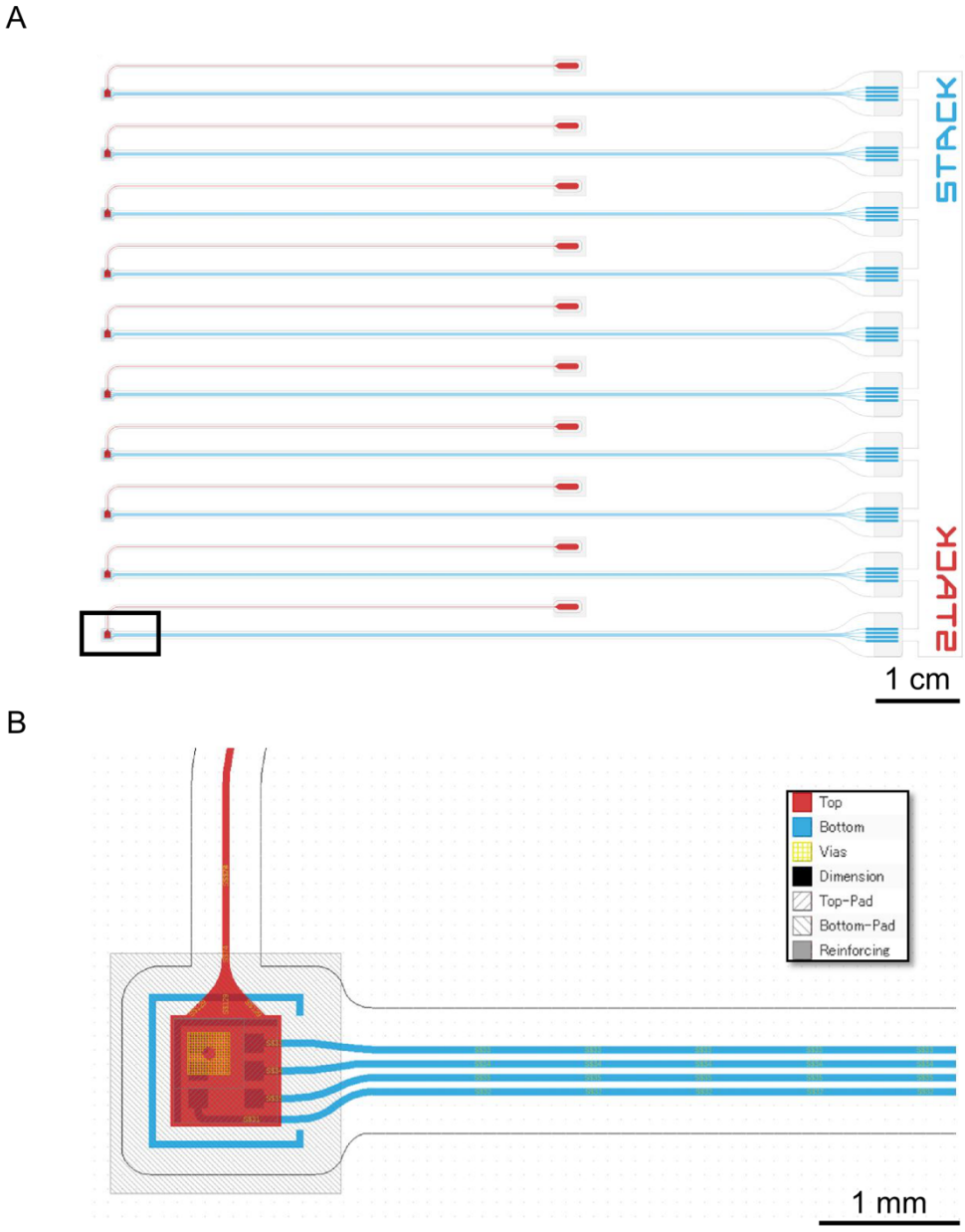

Fig. S2. Layout of the device interposer: (*A*) an array of interposers, with each having electrical connections for both with and without the AMP module and (*B*) an enlarged layout image of the individual interposer (module area). We design the interposer with electrical connections for both with (blue interconnections) and without (red interconnection) the AMP module for the recording comparison using the same electrode module.

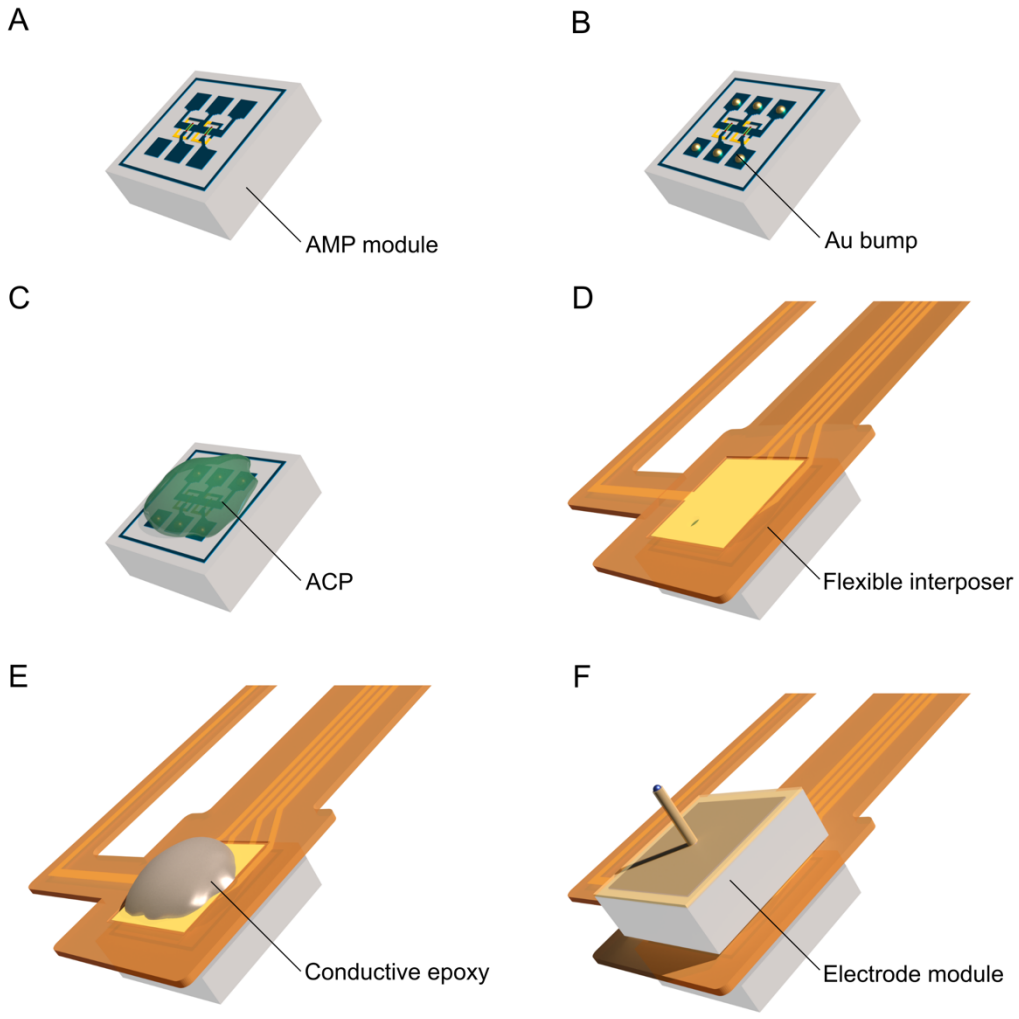

Fig. S3. Assembly procedure of the STACK device: (*A*) AMP (NMOS source follower) module (1 × 1 mm^2), (*B*) gold bumps formed on the pads of the AMP module, (*C*) anisotropic conductive paste (ACP) dipped on the AMP module, (*D*) AMP module mounted on the flexible interposer by flip-chip bonding (MODEL1300, HiSOL, Inc.), (*E*) conductive epoxy (CW2400, CircuitWorks) dipped on the other sided pad of the interposer, and (*F*) electrode module (1 × 1 mm^2) mounted on the interposer via the conductive epoxy.

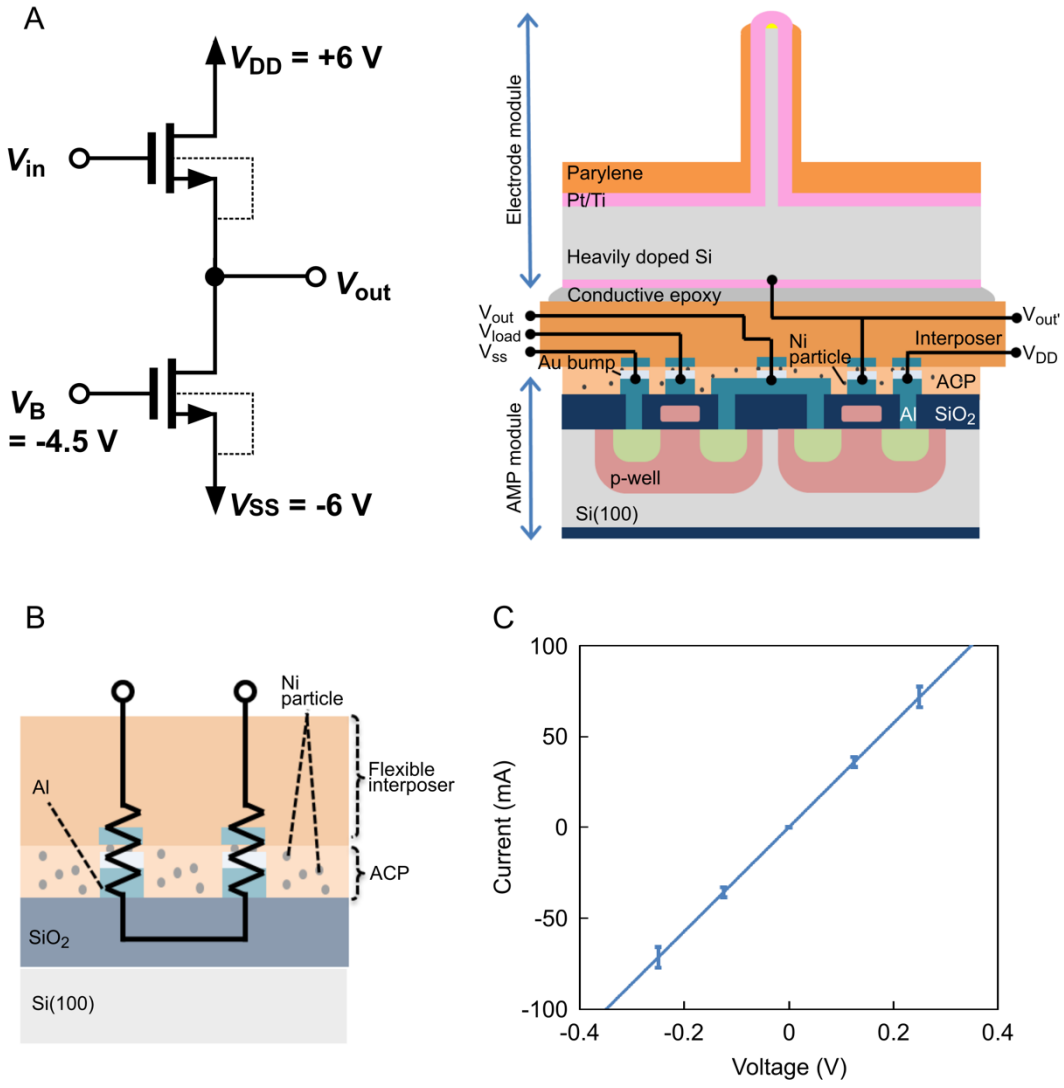

Fig. S4. Assembled STACK device. (*A*) Equivalent circuit of the STACK device, (*B*) cross-sectional schematic of the packaged STACK device (electrode module/interposer/AMP module), and (*C*) electrical properties of the interfaces between the bonding pads of the interposer and the AMP module.

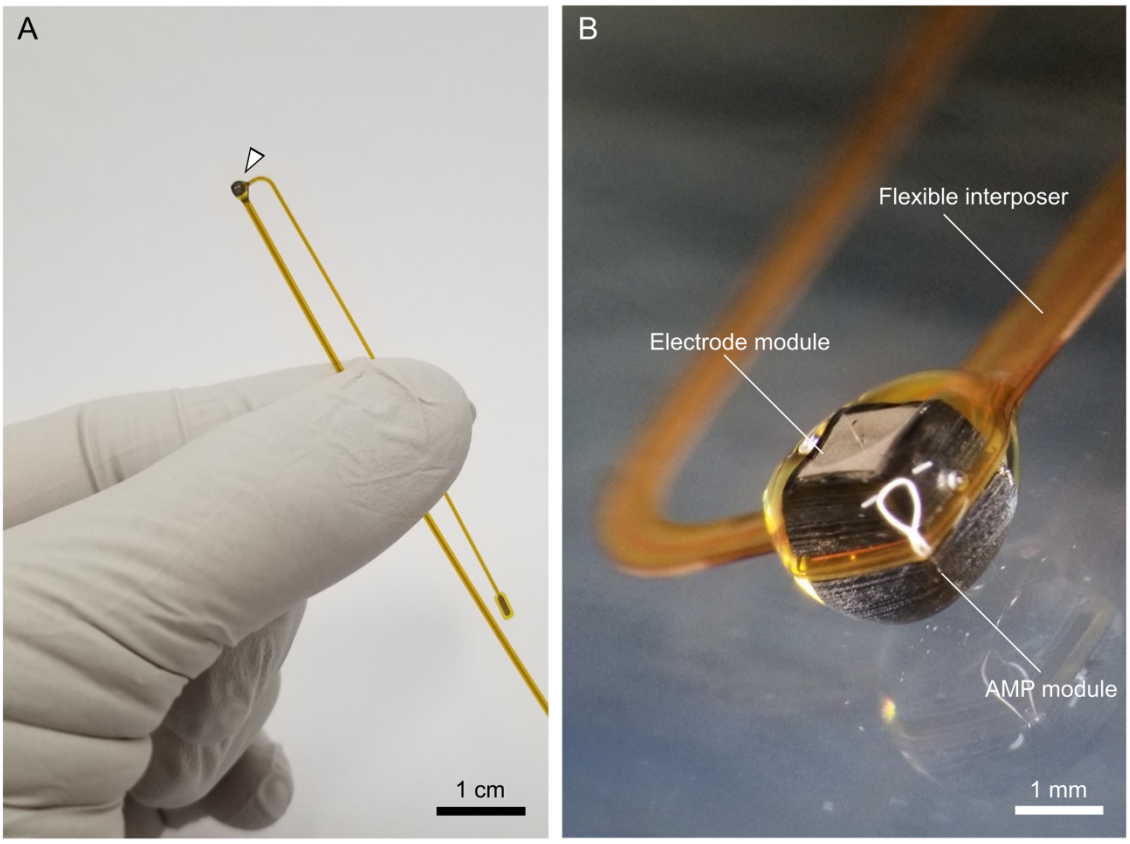

Fig. S5. Encapsulated STACK device with insulating resin. Overall device (*A*) and enlarged image (*B*) of the STACK device. Both modules (electrode and AMP) of Si are encapsulated with insulating ultraviolet curable resin, except for the needle portion in the electrode module. The STACK device consisting of electrical connections for both with AMP and without AMP is used in the in vivo recordings (Fig. 4 and 5, in Main Manuscript).

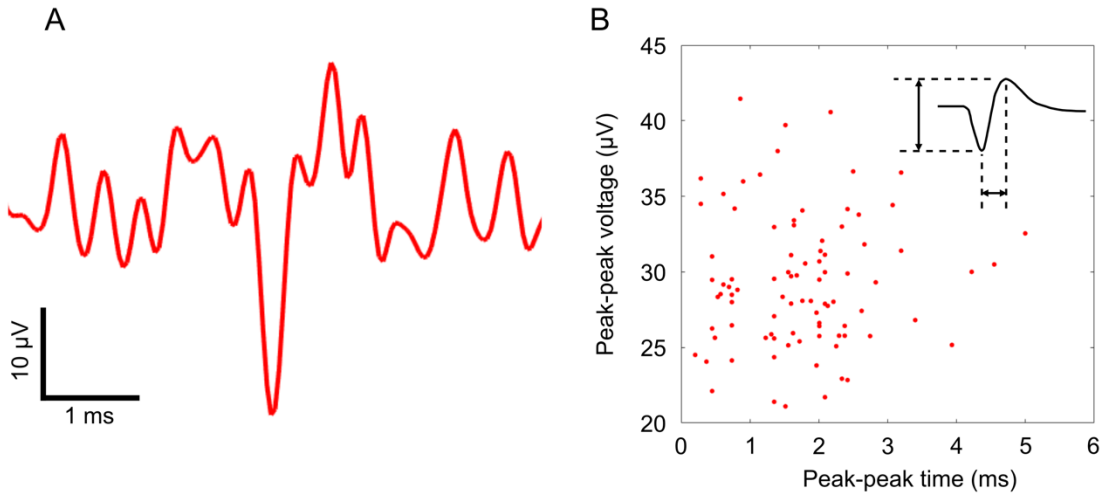

Fig. S6. High-frequency band signals recorded via the needle electrode with the AMP module. (*A*) Signal waveform of a single trial (filtering = 500–3,000 Hz). (*B*) Amplitude and period from peak-to-peak of all spikes. The thresholds used for spike signals were 3× the SD (σ) of the mean signal −0.5 to −1.0 s before the stimulus onset.

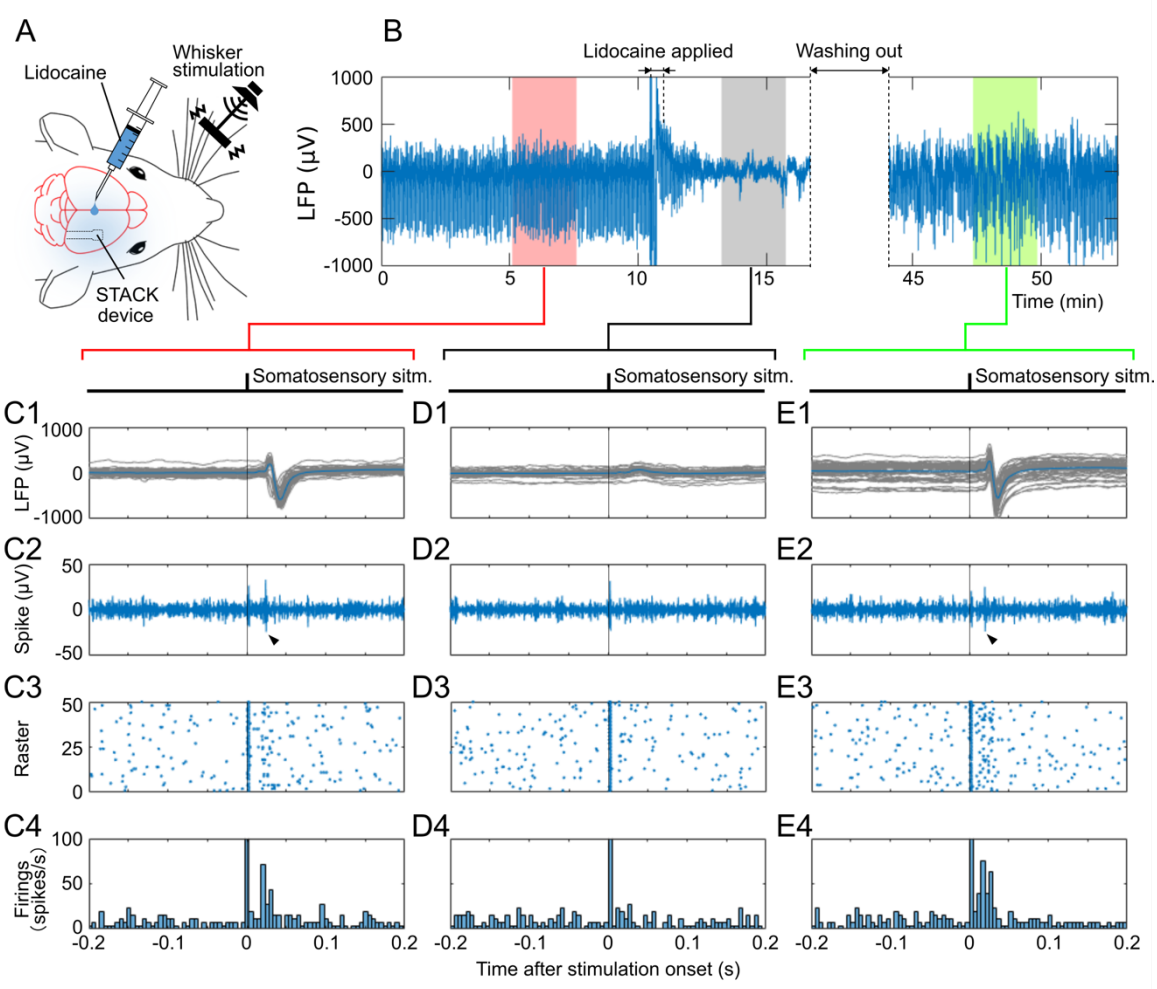

Fig. S7. Pharmacological block of neuronal activity. (*A*) Schematic of the in vivo recording using a mouse. We use lidocaine for the pharmacological block of neuronal activity. The microneedle-electrode of the STACK device penetrated the somatosensory cortex (S1B) of an anesthetized mouse. During the recording, the mouse's whiskers were stimulated, while lidocaine was typically applied to the S1B at ~ 11 s, and then the area of the cortex was washed out with saline for ~30 min. (*B*) Low-frequency band signals (filtering = 1–300 Hz) recorded using the STACK device during the recording period. (*C*, *1*–*4*) Signals recorded before the lidocaine application (5–7.5 min): average waveform of the low-frequency band signals (filtering = 1–300 Hz, n = 50 trials) recorded (*C*, *1*), high-frequency band signal waveform from a single trial (filtering = 500–3,000 Hz) (*C*, *2*), and raster plot diagrams (*C*, *3*) and peristimulus time histograms (PSTHs) taken from these signals. (D, *1*–*4*) Signals recorded after the lidocaine application (13.5–16 min). (E, *1*–*4*) Signals recorded after the washing out the area of the cortex with saline for ~30 min (47.5–50 min). All detection thresholds in high-frequency band signals were 3× the SD (σ) of the mean signal −0.5 to −1.0 s before the stimulus onset.

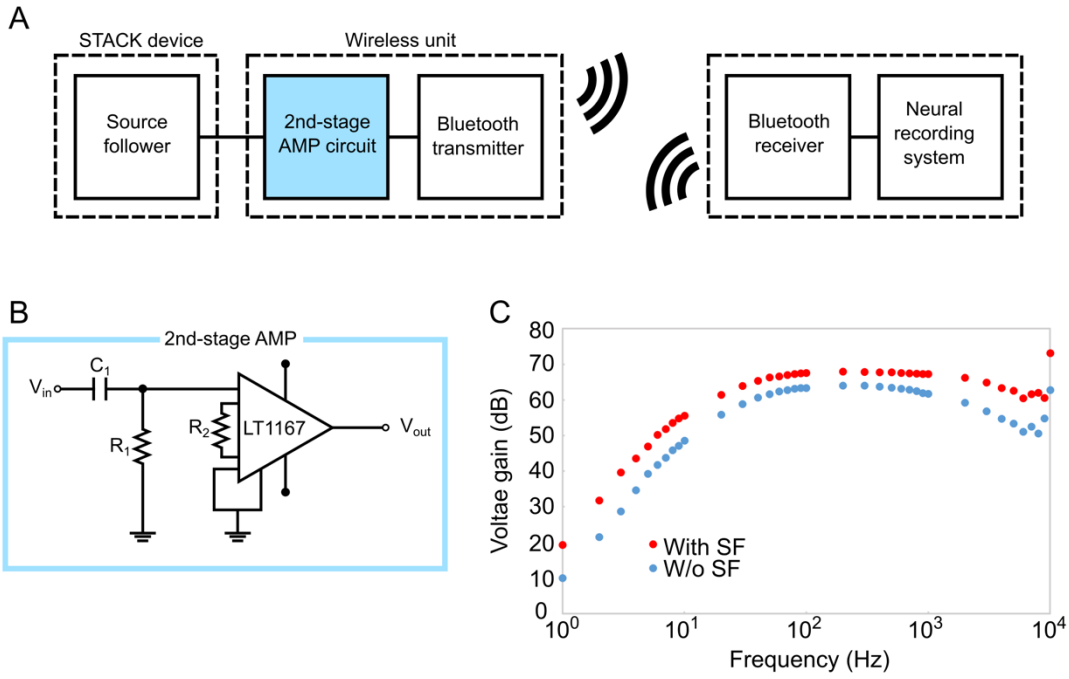

Fig. S8. Wireless neural recording system. (*A*) Block diagram of the wireless recording system, (*B*) schematic of the 2nd-stage amplifier (AMP) circuit, and (*C*) measured transfer function of the wireless neural recording system with and without AMP module of source follower (SF).

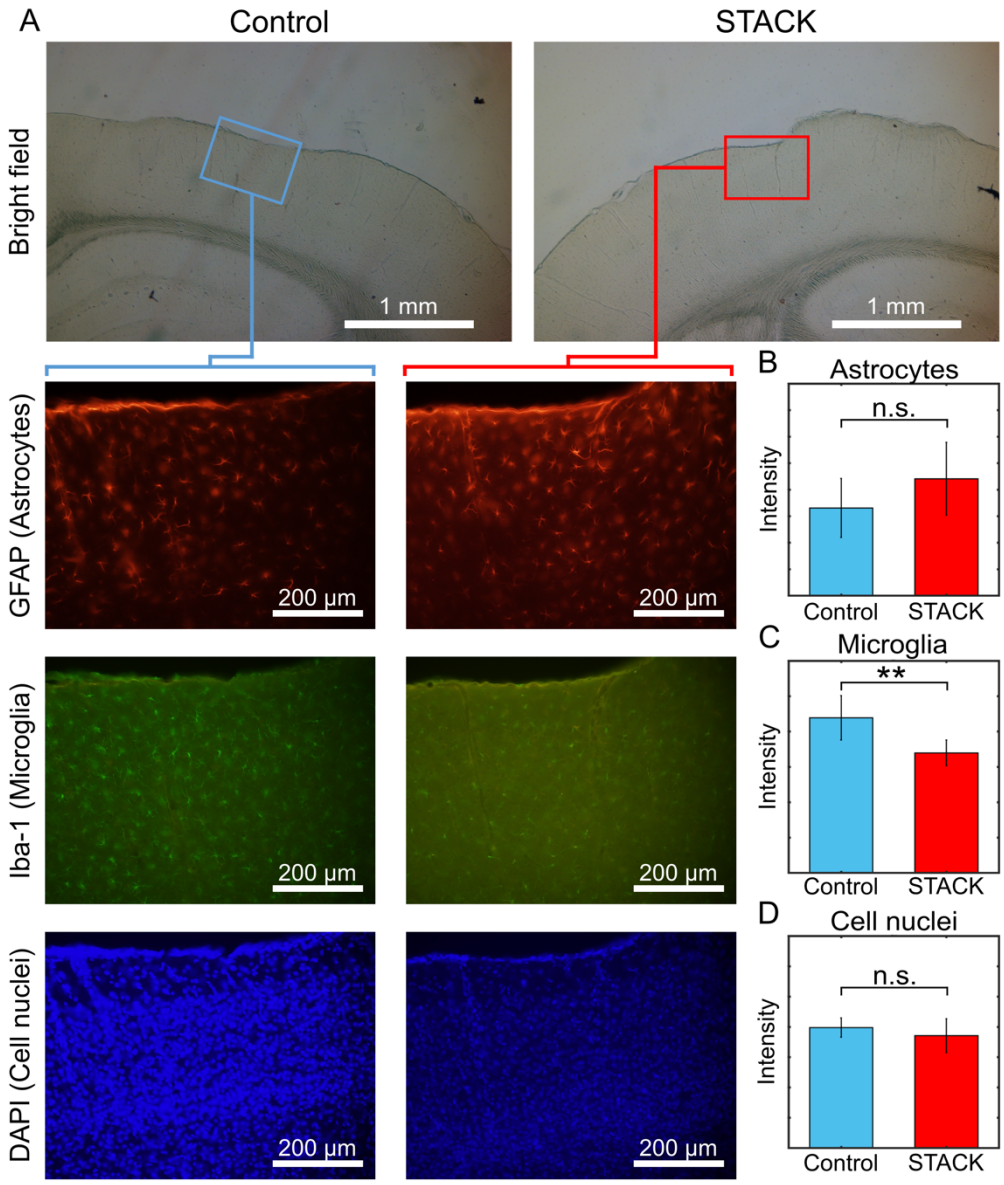

Fig. S9. Immunohistochemistry of tissue responses with and without STACK device implantation. (*A*) Tissue responses in mouse's visual cortex (coronal section) two weeks after without (left panel, "Control") and with (right panel, "STACK") the implanted STACK device. Tissues were labeled for reactive astrocytes (GFAP), microglia (Iba-1), and cell nuclei (DAPI). The STACK device has a surface area of 1 × 1 mm^2 and a height of 1 mm, consisting of a <3-µm-diameter and 400-µm-length needle-electrode. (*B–D*) Quantitative comparison between with and without the STACK device using fluorescent intensity in the 0.15-mm^2 dimensions: (*B*) reactive astrocytes, (*C*) microglia, and (*D*) cell nuclei, taken from 6 slice samples for each cell type. Asterisk denotes a significant difference; ** $p < 0.01$, n.s.: not significant (t-test).

References

1. Y. Kubota, *et al.*, Long nanoneedle-electrode devices for extracellular and intracellular recording in vivo. *Sensors Actuators, B Chem.* **258**, 1287–1294 (2018).